Computer Modeling Analysis for Enediyne Chromophore–Apoprotein Complex of Macromolecular Antitumor Antibiotic C-1027

Yasushi Okuno, Masami Otsuka, and Yukio Sugiura*

Institute for Chemical Research, Kyoto University, Uji, Kyoto 611, Japan

Received January 19, 1994®

On the basis of the van der Waals and electrostatic potential energy calculations and energy minimization (EM), a model for the apoprotein–chromophore complex of C-1027 has been constructed by docking the apoprotein (Apo-C1027) and the chromophore (C1027-Chr). The model of the apoprotein–chromophore complex also suggests the most probable stereochemistry of the chromophore (8*R*,9*S*,13*R*,17*R*), specific interactions between Apo-C1027 and C1027-Chr, and the origin of the stabilization of the chromophore by the apoprotein. The acetylenic bond of C1027-Chr appears to be stabilized by (1) hydrophobic interactions with the bottom of the pocket of Apo-C1027, (2) orbital interaction with Cys36-Cys45 disulfide bond, (3) van der Waals contact with Pro76, and (4) $\pi-\pi$ stacking with the benzene moiety of the chromophore. In this model, molecular dynamics (MD) simulation of the chromophore indicates that the acetylene bond distance (C2–C7) of the apoprotein-bound chromophore is longer than that of the unbound chromophore.

Introduction

A new antitumor antibiotic C-1027, isolated from a culture filtrate of *Streptomyces globisporus* C-1027, shows extremely potent antineoplastic activity against some cultured human cancer cells,[1] and its biological activity has been associated with its ability to cause strong DNA cleavage.[2] The antibiotic is composed of an apoprotein (Apo-C1027) and an associated nonprotein chromophore (C1027-Chr).[3] The apoprotein is a single polypeptide chain of 110 amino acid residues cross-linked by two disulfide bonds (Figure 1),[4] and the homology of the amino acid sequences between C-1027 and actinoxanthin is approximately 93%. The chromophore is extremely unstable in the protein-free state.[5] The chemical structure of C1027-Chr except for the absolute stereochemistry of C8, C9, C13, and C17 was recently determined (Figure 2).[6] This novel chromophore containing a 9-membered enediyne core is responsible for the DNA cleavage reaction of C-1027.[2] The Apo-C1027 plays an important role to stabilize its labile C1027-Chr.[7] Indeed, C-1027 belongs to a chromoprotein family which includes actinoxanthin (AXN),[8] auromomycin (AUR),[9] neocarzinostatin (NCS),[10] and kedarcidin.[11] Very recently, the crystal structure of NCS apoprotein–chromophore complex was published.[10b] The chromophore–apoprotein interaction mode of C-1027 will be distinct from that seen in NCS, however, because there are significant differences in the chemical structures of the chromophore and in the primary structures (47% homology) of the apoprotein between C-1027 and NCS.

Experimental studies of C-1027 are more difficult than those of NCS because of intense lability of C1027-Chr. Therefore, no information about three-dimensional (3D) structure of C-1027 have been reported to date. In such a situation, we investigated 3D interactions between C1027-Chr and Apo-C1027 by calculating van der Waals and electrostatic potential energies, based on the following principles.[12] A guest molecule and binding site of the host form a stable complex when the total interaction energy is lower than the sum of the molecular energies of each isolated component. In other words, two molecules must geometrically provide complementary surfaces to each other in the binding orientation, and when the energy of interaction is minimiized, local regional intermolecular forces are also complementary. The modeled complex provides insights into the specific interaction between C1027-Chr and Apo-C1027 that are unique to this complex and also suggests mechanistic aspects for the stabilization of C1027-Chr by Apo-C1027.

Methods and Results

Modeling of C-1027 Apoprotein. By using Polygen's QUANTA/CHARMm[13] software, a model for the 3D structure of Apo-C1027 was obtained in the following manner. Into the atomic coordinates of AXN deposited in the Brookhaven protein data bank,[7,14] the side chains for seven amino acid residues were replaced and two amino acids were inserted by the Protein Design module. The main chain atom coordinate of the loop containing the inserted residues was copied from the NCS *X*-ray structure.[10b] To avoid the generation of an excessive compact structure by energy minimization, the steepest descent method[15] was used. The preliminary structure was optimized until an RMS gradient force of less than 0.1 kcal/(mol/Å) was reached. The refined Apo-C1027 model ws remarkably similar to the structure of Apo-AXN[14] as expected from its high homology (93%).

The 3D structure of Apo-C1027 consisted of two structural units of different size which form the chromophore binding pocket (Figure 3). A large, flattened cylinder-shape unit contains two groups of antiparallel β-sheets. The external group is composed of three β-strands, S1 (Ser4-Pro8), S2 (Ser17-Val22), and S5 (Phe63-Arg68). The internal group forms the floor of the pocket and is composed of four strands, S3 (Thr30-Val39), S4 (Ser52-Asp56), S6 (Asn92-Asn97), and S7 (His104-Ala106). On the other hand, a small unit of three antiparallel β-strands makes up the sides of the

* To whom correspondence should be addressed.
® Abstract published in *Advance ACS Abstracts*, June 1, 1994.

0022-2623/94/1837-2266$04.50/0

Figure 1. Amino acid sequences of apoproteins of C1027, NCS, and AXN. Homology alignment between Apo-C1027 and Apo-AXN is indicated by a box. The lines of Cys-Cys show the disulfide bond common in three apoproteins.

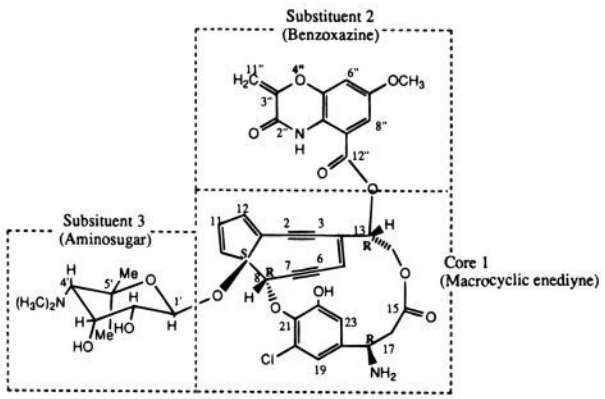

Figure 2. Chemical structure of the C-1027 chromophore (C1027-Chr). The stereochemistry shown is predicted from this study.

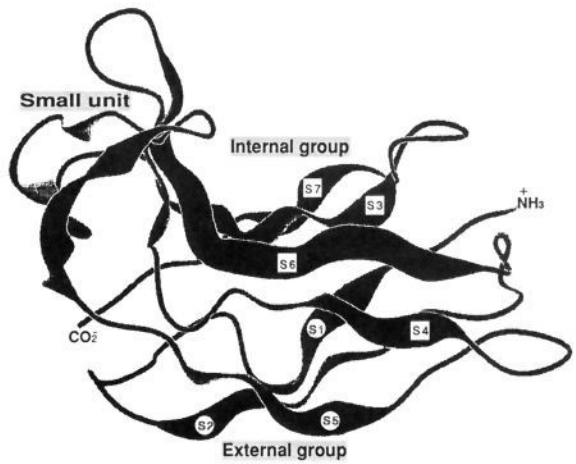

Figure 3. Ribbon presentation of Apo-C1027. The letters (S3,S4,S6,S7) and (S1,S2,S5) surrounded by squares and circles show internal sheet and external sheet, respectively. The other sheets constitue the small unit.

pocket, s1 (Cys36-Pro47), s2 (Ser70-Ser74), and s3 (Gly82-Asp85). The pocket is lined with amino acid residues of Tyr32-Ser52, Thr72-Pro80, and Ala89-Ala106 (Figures 4 and 5), which can interact with C1027-Chr. It is important to note that five (Thr72, Ser74, Glu77, Ala89, and Asp101) residues of the seven replacements are among the amino acid residues forming the pocket. The five residues are characteristic of Apo-C1027 and hence may play an essential role for the binding specificity of its chromophore. Hydrophobic amino acid residues, Ile33-Ala34, Leu93-Gly96, and Leu102-Gly103, located in the bottom of this pocket, probably take part in hydrophobic interactions with C1027-Chr (Figures 4 and 5).[7]

Modeling of C-1027 Chromophore. C1027-Chr possesses a macrocyclic structure which consists of a 9-membered 1,5-diyn-3-ene core and a 16-membered cyclic bridge, together with benzoxazine and amino sugar moieties as side chains (Figure 2).[5,6] However, its absolute stereochemistry except for that of the amino sugar moiety[6c] and the apoprotein-bound conformation of C1027-Chr have not been determined. In order to decrease the complexity of the conformational search, the chromophore was first divided into the macrocyclic enediyne core 1, substituent 2 (the benzoxazine), and substituent 3 (the amino sugar), and then the conformation of each fragment was investigated.

The two substituents, 2 (C12″-OH) and 3 (C1′-OH) (Figure 2), were constructed by the 3D construction tool of QUANTA.[6] These models were minimized to an RMS gradient force of ≤ 0.001 with the steepest descent method followed by ABNR (Adopted-Basis Newton-Raphson) methods.[13] On the other hand, the enediyne core 1 (1:C9-OH, C13-OH) has four asymmetric centers of unknown absolute stereochemistry at C8, C9, C13, and C17. The relative stereochemistry at C8 and C9 was reported as trans by the NMR data.[6a] The macrocyclic structure produces two planes of asymmetry, i.e., one for the benzene ring and another for the 9-membered enediyne moiety. The stereochemistry of C8 dominates the rotation of the chiral enediyne plane around the C4−C3 axis. We chose two stereoisomers

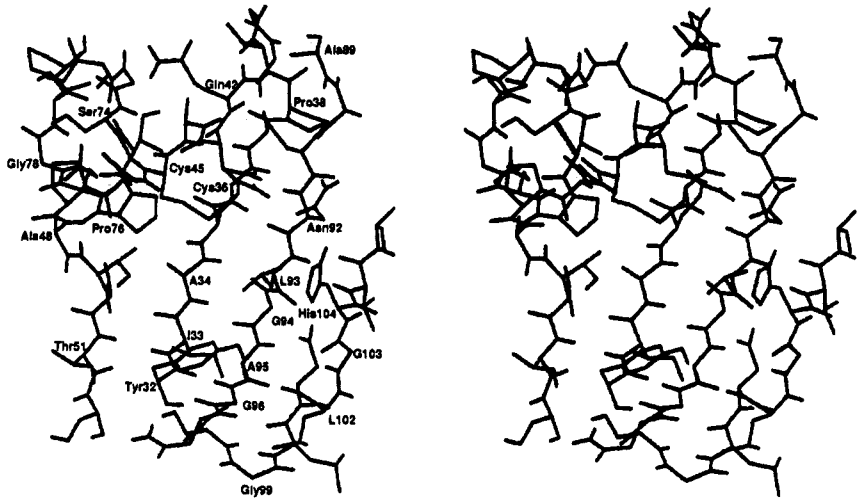

Figure 4. Stereoview of binding pocket of Apo-C1027 for C1027-Chr. One letter codes indicate the residues forming the hydrophobic bottom.

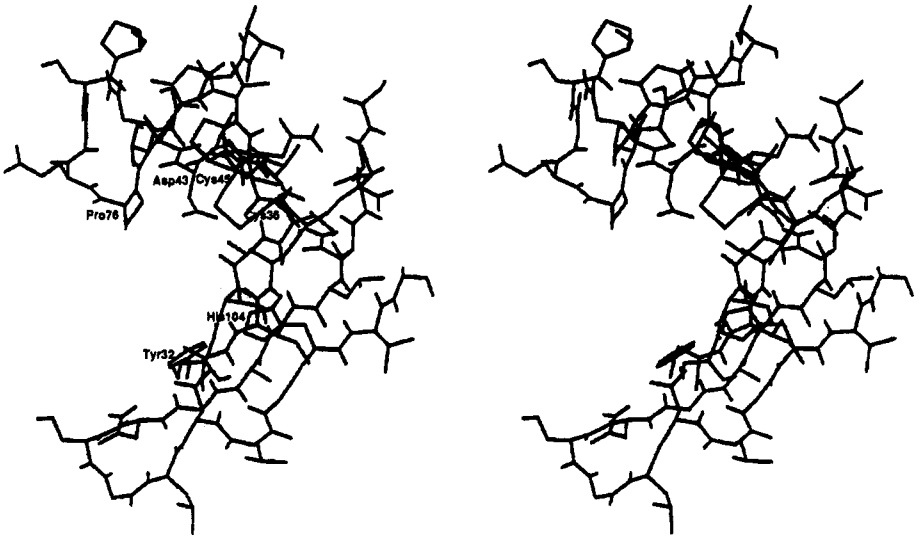

Figure 5. Stereoview of binding pocket of Apo-C1027 for C1027-Chr. This point of view differs from that of Figure 4.

among the all possible 32 (=2^5) isomers as follows. Since the conformation of the macrocyclic core 1 appeared to be influenced significantly by altering the stereochemistry of C8 and C9, we decided to examine the two stereoisomers concerning C8 and C9 (8*R*,9*S* and 8*S*,9*R*), and the stereochemistry of C13 and C17 was tentatively fixed as 13*R*,17*R* for the initial calculation. Since the labile enediyne moiety of the chromophore is stabilized by the apoprotein, the adequate conformation of the enediyne core 1 in the pocket must have the lowest energy.[16] In order to overcome the local minima problem in locating the lowest energy conformation, the simulated annealing[17] tool, Grid Scan Search, in QUANTA was used. This is the full conformational search tool of C1027-Chr that generates 1296 (=6^4) conformers by the rotation of the bonds C4—C13, C14—O, C15—C16, and C21—O in 60° intervals using CHARMm parameters. Through this search, the most stable conformer was selected among several ones. In the insertion of these two steeoisomeric enediyne core 1 models into the pocket of the apoprotein, favored configuration at C8, C9, C13, and C17 and the asymmetry of the benzene ring plane were searched by considering contacts between the enediyne core 1 and the amino acid residues of Apo-C1027 as described in the following sections. Finally, the substituents 2 and 3 were connected to the enediyne core 1 in the pocket of C1027-Chr by exploration of their favored binding sites and orientations.

Binding-Site Exploration. In order to search the favored binding site for C1027-Chr in the pocket of Apo-C1027, van der Waals and electrostatic potential energies were computed by Probe Interaction Calculation in QUANTA on an IRIS 4D/35TG graphic workstation. The switch function was used in this calculation for the van der Waals and electrostatic interactions between 11.0 and 14.0 Å with a 15.0-Å cut list. The carbon atom of C11 (or C12) and the chloro group of the core 1, and also the ring oxygen, the ring nitrogen, and the methoxyl carbon atoms in the substituent 2 were seleted as probes to search the potential enviroment in the pocket. No atoms of the amino sugar were selected, because the amino sugar of C1027-Chr is not expected to interact with Apo-C1027 just as that of NCS-Chr located out of the pocket.[10b,18] The atomic charges of C11 or C12 carbon, the chlorine, the ring oxygen, the ring nitrogen, and the methoxyl carbon screened to 0, −0.2, −0.37, −0.35, and +0.15, respectively. This calculation gave the empirical energy (the sum of both van der Waals and electrostatic energies) between the probes and the Apo-C1027 pocket. The lowest energy, attractive, regions of the probes in the pocket were displayed as

Table 1. Favored Binding Sites and Empirical Energy Values for Each Probe Atom of C1027-Chr

probe	energy (kcal/mol)	residues (forming favored binding sites)
	Core 1	
C11 or C12	−3	Asn46 Pro47 Pro76 Glu77
	−3	Ala34 Leu93 Gly94
chloro group	42	Tyr32 Ala34 Ala50 Gly94
	Substituent 2	
ring oxygen	35	Asn92 His104 Val105 Ala106
ring nitrogen	35	Asn92 His104 Val105 Ala106
methoxyl carbon	−28	Cys36 Asp43 Asn92 His104
	−28	Gly94 Ala95 Asp101 His104

energy contours maps, e.g., the pink brick regions in Figure 6a. Table 1 summarizes the obtained lowest empirical energy values for each probe atom of C1027-Chr, together with the favored binding residues. For example, the chloro group of the core 1 was placed near the phenolic alcohol of the core 1 situated out of the hydrophobic pocket. The rotating angle of the chiral plane of the benzene ring was thus optimized. The ring oxygen and nitrogen atoms of the substituent 2 are able to form hydrogen bonds with Asn92 and His104 residues. The C11 (or C12) and methoxyl carbon atoms presented two possible binding sites. These more favorable sites, (Asn46 Pro47 Pro76 Glu77) for C11 (or C12) and (Gly94 Ala95 Asp101 His104) for the methoxyl carbon, were determined by electrostatic potential field calculation as follows.

In order to clarify the orientations of the fragments 1 and 2 in the pocket, the electrostatic potentials (maximum 16.78 kcal/mol; minimum −45.42 kcal/mol) at van der Waals surface of the Apo-C1027 pocket were calculated by using Solvent Surface Calculation in QUANTA. The electron distribution used in this calculation was obtained by CHARMm empirical calculation. The obtained potential field gave a clear picture for the distribution of molecular electrostatic potential of Apo-C1027 pocket (Figure 6a). The binding pocket consisted mainly of a negative potential region (n3) and a positive potential region (p3). Outside these regions, there were a small positive potential region (p4) formed by Asn92, Val105, and Ala106, and a small negative potential region (n4) formed by Pro76 and Glu77. In a similar manner, electrostatic potential surfaces of the macrocyclic enediyne core 1 nd the substituent 2 were estimated (Figure 6b). The core 1 and the substituent 2 showed the potential values of maximum 18.97 and minimum −19.47 kcal/mol, and maximum 14.75 and minimum −11.40 kcal/mol, respectively. The substituent 2 was divided into positive (p2) and negative (n2) potential regions by a imaginary plane that is perpendicular to the benzoxazine ring and crosses C5″ and C12″. The core 1 was also separated into positive (p1) and negative (n1) potential regions by a imaginary plane that is nearly perpendicular to 16-membered ring and contains C13 and C18. As to binding of two molecules, the electrostatic potential pattern of the interfacial surface should ideally be complementary with adjacent areas of positive and negative potential, reflecting an attractive electrostatic forces. Therefore, the pattern matching of the electrostatic fields of the binding surfaces of the two molecules, Apo-C1027 and the chromophore, was investigated from the favored binding residues in the previous calculation. The positive (p2) and the negative (n2) potential regions of the substituent 2 corresponded well to the negative (n3) and the small positive (p4) potential regions of the Apo-C1027 pocket. In addition, the positive (p1) and the negative (n1) potential regions of the core 1 matched the negative (n3) and the positive (p3) regions of the pocket.

Model Building of C-1027 Apoprotein–Chromophore Complex. On the basis of the above-mentioned results, the enediyne core 1 and the substituent 2 of C1027-Chr docked into the protein. In the course of locating the enediyne core 1 in the pocket, the stereochemistries of C8, C9, C13, and C17 and rotational asymmetry of the benzene plane were defined as follows. Two stereoisomers of the core 1 (8*R*,9*S* and 8*S*,9*R*) were respectively located in the pocket. The 8*S*,9*R* isomer points the hydroxyl group at C9, which has to hold the amino sugar 3 toward the bottom of the pocket (8S9R isomer). Namely, there was no space to accommodate the amino sugar moiety 3. Only in the case of the 8*R*,9*S* isomer could an agreeable orientation of the C9 hydroxyl be obtained. By considering the spatial relationship of the core 1 and the substituent 2, the stereochemistry at C13 was defined as *R*. The amino group on the C17 was pointed outward to avoid a bad contact with the apoprotein, and hence the configuration of C17 was determined as *R*. Therefore, the most probable stereochemistry of C1027-Chr was deduced to be 8*R*,9*S*,13*R*,17*R*. The rotational geometry of the benzene ring plane was obtained so as to make the hydrophilic phenolic hydroxyl group away from the pocket as described in the previous section.

The connective operation of the enediyne core 1 with the substituent 2 was determined by placing the two fragments in positions where the interaction energy between fragments 1 and 2 and the apoprotein became as small as possible by using the continuous energy facility in QUANTA. The enediyne core 1 and the substituent 2 were successively connected in the pocket. The substituent 3, just as the amino sugar of NCS,[10b,18] is situated out of the pocket of Apo-C1027. After the connection to the core 1 in the pocket, the substituent 3 was located at an appropriate position by using the Spin tool in QUANTA. This tool was used to automatically rotate the bonds, C9—O and O—C1′, to search for a conformation in which the amino sugar contacts against the core 1 and the apoprotein were minimized. The unrefined chromophore structure had a few improper bond lengths and bond angles at the connecting site. The whole structure of C-1027 including the apoprotein and the unrefined chromophore was then subjected to minimization by CHARMm until the RMS gradient force became less than 0.1 kcal/(mol/Å) using the steepest descent method followed by the conjugate gradient method. Main chain atomic coordinates of the apoprotein in the optimized complex retained their original positions for the most part and only the conformations of several side chains in the binding site underwent any significate changed. The conformation of the chromophore also changed slightly. Figures 7 and 8 show the refined structure for the chromophore–apoprotein complex of C-1027.

Molecular Dynamics of Apoprotein-Free Chromophore. In order to compare the conformation of C1027-Chr in the bound and unbound states, the behavior of the chromophore was simulated using CHARMm molecular dynamics (MD). The conformation

Table 2. Characteristic Interatomic Distance between the Chromophore and the Apoprotein in the C-1027 Complex Model

chromophore	apoprotein	distance (Å)
Core 1		
C2	Pro76 Cα	3.419
	Cys45 Sγ	3.839
C3	Pro76 Cγ	3.453
	Cys45 Sγ	3.669
C6	Cys36 Sγ	3.066
	Cys45 Sγ	3.509
C7	Ala34 Cβ	3.237
	Cys36 Sγ	3.853
hydrogen of amino group	Tyr32 O(−H)	3.075
	Asp101 Oδ	4.925
chlorine	Ile33 Cα	3.876
center of endiyne-moiety plane	benzene ring[a]	3.916
Substituent 2		
oxygen of C3″−O	Asn92H(−Nδ)	2.966
	His104H(−Nω)	2.942
C2″=O	Pro38 Cβ	3.228
	Asn92 H(−Nδ)	3.285
hydrogen of methoxyl group	Gly94Cα	3.490
carbon of N1″−H	Asp43Oδ	2.784
Substituent 3		
nitrogen of dimethylamino group	Glu77 Oε	7.775

[a] Distance between the centers of the endiyne-moiety plane and the benzene ring of C1027-Chr.

of the chromophore taken from the apoprotein−complex was used as the starting structure of MD simulation. The following CHARMm detailed dynamics simulation was performed throughout this study. In a 3.0-ps heating phase, the temperature was raised to 300 K in steps of 0.05 ps. This was followed by an equilibration phase in which the velocities were allowed to rescale over the next 7.0 ps in steps of 0.05 ps to stabilize the system within 300 ± 10 K. The simulation phase was continued for another 20 ps where the velocities were allowed to rescale every 0.05 ps. Nonbonded interactions (van der Waals and electrostatic interactions) were computed with a switch truncation between 11.0 and 14.0 Å with a cutoff distance of 15.0 Å. Figure 9 shows a plot of the interatomic distance for the Bergman reaction centers as a function of the simulation time. The MD simulation yielded an average distance of 3.10 Å between the reactive centers, C2−C7. The distance was evidently shorter than that of the apoprotein-bound chromophore (3.16 Å).[19]

Discussion

Interaction between Chromophore and Apoprotein. Table 2 shows the characteristic contacts between amino acid residues of the protein and functional groups of the chromophore. The benzoxazine moiety 2 is located in a deep pocket consisting of Pro38, Asp43, Asn92, Gly94, and His104 (Figures 7 and 8). Hydrogen bonds mainly contribute to these interactions. The ring oxygen atom (C3″-O) of the substituent 2 forms a hydrogen bond with His104 and Asn92 side chains. The H(−N1″) atom and the O(=C2″) atom are also close to the oxygen atom of Asp43 side chain and the hydrogen atom of Asn92 side chain, respectively, and are capable of forming hydrogen bonds. The methoxyl groups is in van der Waals contact with the α-carbon atom of Gly94, suggesting that the hydrogen bonds formed by the benzoxazine moiety 2 play an important role for complex formation of C1027-Chr and Apo-C1027. In addition, the release of C1027-Chr from Apo-C1027 is predicted to depend on pH analogous to the release of NCS-Chr from Apo-NCS.[20]

Of special interest is the fact that the enediyne core 1 enjoys a good fit in the center of the pocket. The carbon atom of C7 and the chlorine atom are located in the vicinity of Ala34 and Ile 33 residue. The enediyne and benzene moieties are likely to face down toward the hydrophobic bottom of the pocket. Presumably, these moieties of the core 1 form hydrophobic interactions with the hydrophobic bottom of the pocket. Indeed, C1027-Chr is extractable from Apo-C1027 by organic solvents.[5] In addition to such hydrophobic interactions, the benzene moiety also forms an aromatic stacking interaction with Tyr32 residue, shown by the distance of 3.916 Å between benzene rings of the core 1 and Tyr32.[7] The C6−C7 acetylenic bond of the core 1 is situate in van der Waals contact with the sulfur atoms of Cys36-Cys45. This disulfide bond probably contributes to stabilize the acetylenic bond of C1027-Chr.[7] The 5-membered ring of Pro76 surrounds the other side of the enediyne core and is in van der Waals contact with the C2−C3 acetylenic bond. An additional salt bridge interaction is observed between the protonated amino group (C17-NH_2) of the chromophore and the oxygen atoms of Asp101 and Tyr32. The amino sugar moiety 3 shows no clear interactions with the apoprotein except for the dimethylamino group (C4′-$N(CH_3)_2$). The protonated dimethylamino group can form a salt bridge with the carboxylate group of Glu77. The hydrophilic amino sugar may contribute to the chromophore−DNA binding rather than apoprotein binding and also may play an essential role as a trigger for release of the chromophore from the apoprotein to DNA. In summary, the core 1 appears to provide a driving force to insert the chromophore into the apoprotein and to release the chromophore from the apoprotein. The benzoxazine moiety 2 contributes to formation and stabilization of the chromophore−apoprotein complex mainly through hydrogen bonds. The amino sugar moiety 3 may play a part as a trigger for the transfer of the chromophore from the apoprotein to DNA.

Previously, we observed that C-1027 is much more reactive in the presence of DNA than in the absence of DNA.[2] On the basis of these observations, we propose a mechanism of C1027-Chr release from Apo-C1027 on DNA binding and cleavage in vitro. When DNA approaches to holo-C1027 (complexed form) in which the chromophore is stabilized by hydrogen bonds and hydrophobic interactions, the hydrophilic amino sugar first interacts to DNA. Next, the regular hydration core of the DNA[21] changes the structure of water on the peripheral part of the pocket, and this affects the structural situation of the apoprotein pocket. The alterations of the hydrophobic surroundings and the local pH in the pocket lead to release of the chromophore from the apoprotein. Since the chromophores of NCS[6,22] and kedarcidin,[11] as well as C1027-Chr, have amino sugars, the same mechanism for the chromophore release may be common to the chromoprotein family. A specific interaction between C-1027 and DNA is now under investigation.

Stabilization of Chromophore by Apoprotein. On the basis of the C2−C7 distance from the MD simulation it is predicted that the chromophore should be more stable in the apoprotein complex when free in

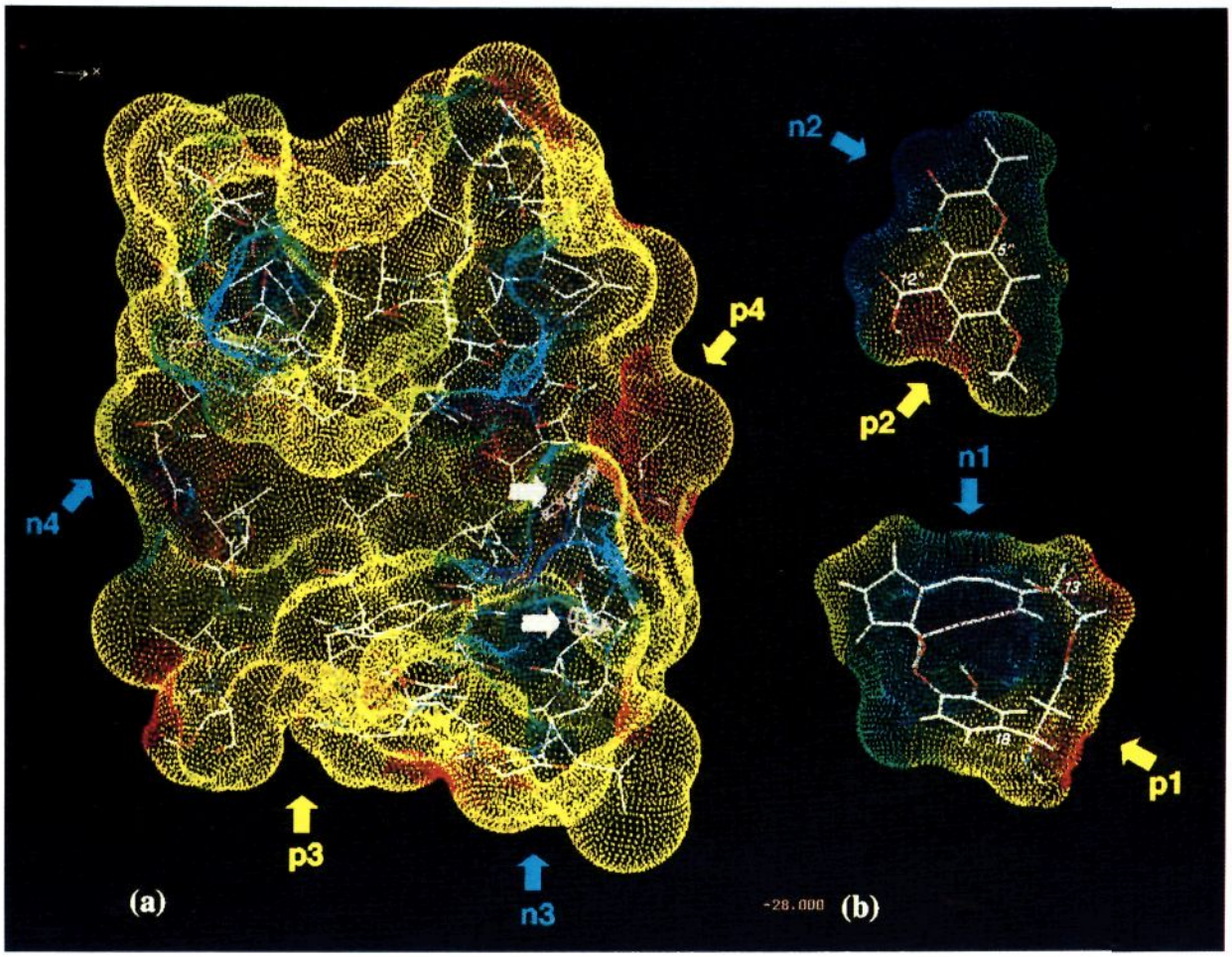

Figure 6. (a) Molecular electrostatic potential at van der Waals surface of binding pocket of Apo-C1027 and the faborable sites of the methoxyl carbon of C1027-Chr. The potential values are represented by colors, stepwise, from red (maximum 16.78 kcal/mol) to blue (minimum −45.42 kcal/mol). This pocket contains mainly two positive regions (p3, p4) and two negative regions (n3, n4). The orientation of the binding pocket is the same as that of Figure 4. The pink arrows show the pink brick regions, the favored binding sites of the methoxyl carbon atom. (b) Molecular electrostatic potential at van der Waals surface of the core 1 (bottom) and the substituent 2 (top). The potential values of the core 1 and the substituent 2 are represented by colors, stepwise, from red (maximum 18.97 and 14.75 kcal/mol) to blue (minimum −19.47 and −11.40 kcal/mol). Both molecules contain positive (p1, p2) and negative (n1, n2) regions, respectively.

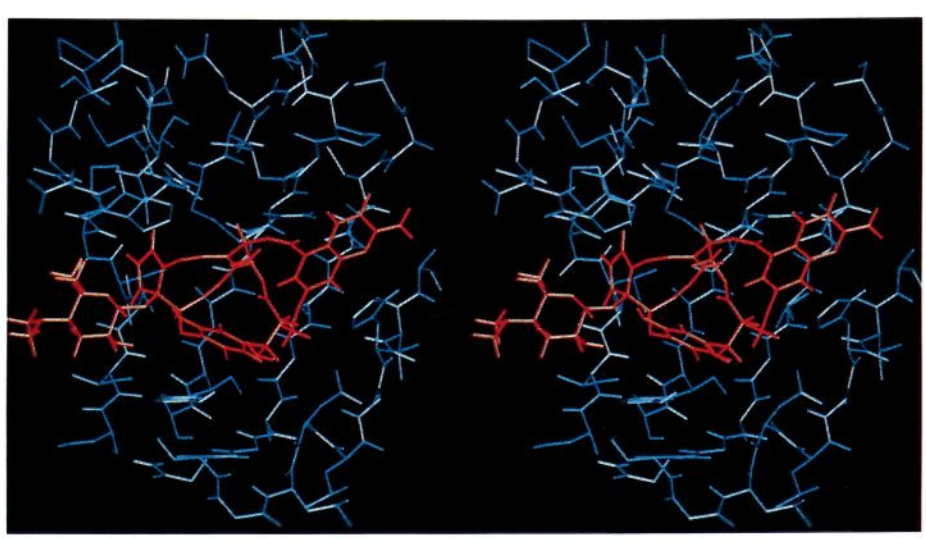

Figure 7. Stereoview of binding site in apoprotein−chromophore complex of C-1027. C1027-Chr and Apo-C1027 are shown in red and blue, respectively. The orientation of the apoprotein is the same as that of Figure 4.

solution, consistent with the fact that C-1027 plays an important role to stabilize the chromophore.[7] The model suggests that the remarkable stabilization of the apoprotein-bound chromophore may be due to the following

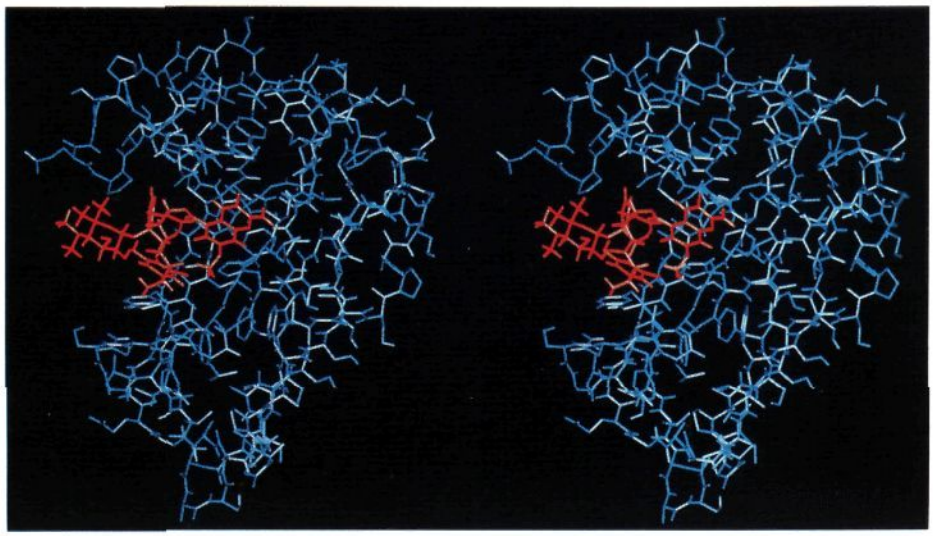

Figure 8. Stereoview of whole structure in apoprotein-chromophore complex of C-1027. C1027-Chr and Apo-C1027 are shown in red and blue, respectively. The orientation of the apoprotein is the same as that of Figure 5.

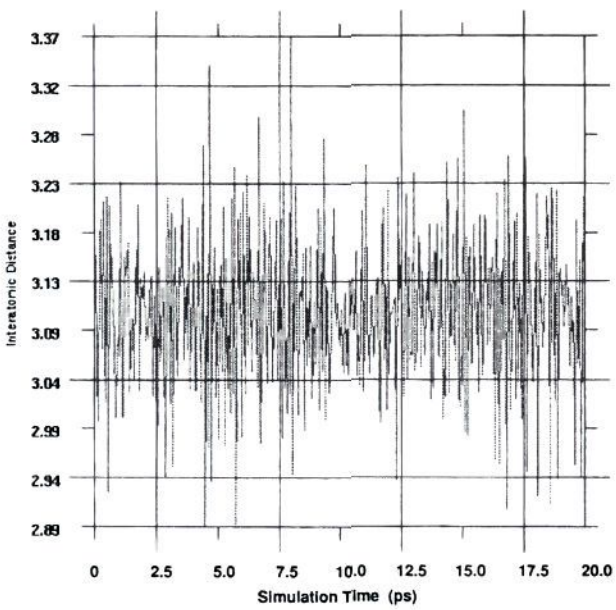

Figure 9. Plot of interatomic distance for Bergman reaction centers (C2–C7) as a function of the simulation time for C1027-Chr.

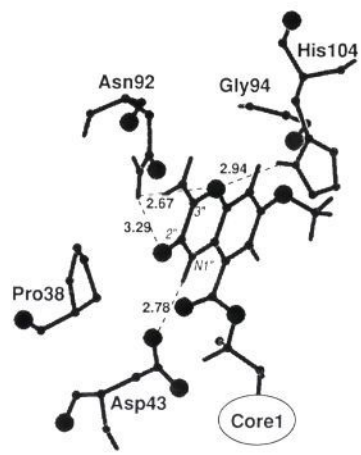

Figure 10. Specific interaction of benzoxazine moiety 2 of C1027-Chr with characteristic residues of Apo-C1027. The dashed line shows hydrogen bond and the number of the line presents its interatomic distance (Å). Large and small closed circles indicate oxygen and carbon (or nitrogen) atoms, respectively.

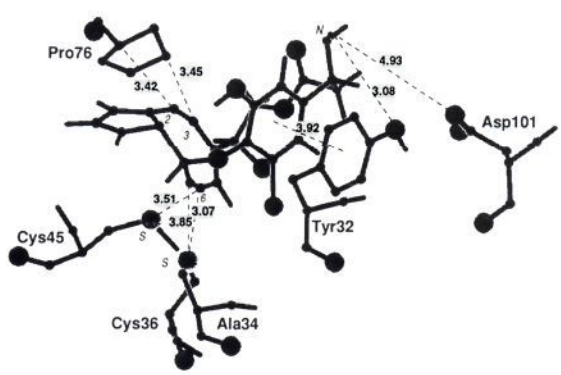

Figure 11. Specific interaction of endiyne core 1 of C1027-Chr with amino acid residues of Apo-C1027. The dashed line shows the important interaction of the core 1 and the number on the line presents its interatomic distance (Å). Large and small closed circles indicate oxygen and carbon (or nitrogen) atoms, respectively.

interactions (Figures 10 and 11): (1) The hydrophobic interactions between the enediyne moiety and the bottom of the pocket of Apo-C1027,[7] (2) The C6—C7 acetylenic bond of the core 1 is located on the disulfide bond (Cys36-Cys45),[7] which probably stabilizes the acetylenic system of C1027-Chr through their orbital HOMO (the enediyne π-system)—LUMO (disulfide σ^* or vacant d orbital) interaction,[18b] (3) The 5-membered ring of Pro76 is in van der Waals contact with the other acetylenic bond (C2—C3), and (4) The enediyne plane formed by the acetylenic bonds of C2—C3 and C6—C7 is approximately parallel to the intramolecular benzene ring plane, and hence π–π stacking interaction is expected between both the planes.

In conclusion, the most probable stereochemistry of C1027-Chr is 8*R*,9*S*,13*R*,17*R*. The rotational geometry of the benzene ring plane makes the hydrophilic phenolic hydroxyl group away from the hydrophobic pocket. The amino group on the C17 is pointed outward to avoid a bad contact with apoprotein. The acetylene bond distance (C2—C7) differs between C-1027 and C1027-Chr. The present study provides valuable information

for specific interactions of the apoprotein with the chromophore in C-1027 antitumor antibiotic.

Acknowledgment. This study was supported in part by a Grant-in-Aid for Scientific Research on Priority Area (06240104) from the Ministry of Education, Science, and Culture, Japan. In this study, computation time was provided by the Supercomputer Laboratory, Institute for Chemical Research, Kyoto University.

Supplementary Material Available: Atomic coordinates for the C-1027 apoprotein–chromophore complex model (16 pages). Ordering information is given on any current masthead page.

References

(1) (a) Hu, J.; Xue, Y.-C.; Xie, M.-Y.; Zhang, R.; Minami, Y.; Yamada, Y.; Marunaka, T. A new macromolecular antitumor antibiotics, C-1027. I. Discovery, taxonomy of producing organism fermentation and biological activity. *J. Antibiot.* (*Tokyo*) **1988**, *41*, 1575–1579. (b) Otani, T.; Minami, Y.; Marunaka, T.; Zhang, R.; Xie, M.-Y. A new macromolecular antitumor antibiotics, C-1027. III. Antitumor activity. *J. Antibiot.* (*Tokyo*) **1988**, *42*, 1294–1298.

(2) Sugiura, Y.; Matsumoto, T. Some characteristics of DNA strand scission by macromolecular antitumor antibiotic C-1027 containing a novel enediyne chromophore. *Biochemistry* **1993**, *32*, 5548–5553.

(3) Otani, T.; Minami, Y.; Marunaka, T.; Zhang, R.; Xie, M.-Y. A new macromolecular antitumor antiobiotic, C-1027. II. Isolation and physico-chemical properties. *J. Antibiot.* (*Tokyo*) **1988**, *41*, 1580–1585.

(4) Otani, T.; Yasuhara, T.; Minami, Y.; Shimazu, T.; Zhang, R.; Xie, M.-Y. Purification and primary structure of C-1027-AG, a selective antagonist of antitumor antibiotic C-1027, from *Streptomyces globisporus*. *Agric. Biol. Chem.* **1991**, *55*, 407–417.

(5) Otani, T.; Minami, Y.; Sakawa, K.; Yoshida, K. Isolation and characterization of non-protein chromophore and its degradation product from antibiotic C-1027. *J. Antibiot.* (*Tokyo*) **1991**, *44*, 564–568.

(6) (a) Otani, T.; Minami, Y.; Yoshida, K.; Azuma, R.; Saeki, M. Structure of an aromatization product of C-1027 chromophore. *Tetrahedron Lett.* **1993**, *34*, 2633–2636. (b) Otani, T.; Yoshida, K.; Minami, Y.; Azuma, R.; Saeki, M. Structure and cycloaromatizatiion of a novel enediyne, C-1027 chromophore. *Tetrahedron Lett.* **1993**, *34*, 2637–2640. (c) Hirama, M.; Iida, K.; Ishii, T. Synthesis and absolute stereochemistry of the aminosugar moiety of antibiotic C-1027 chromophore. *Tetrahedron Lett.* **1993**, *34*, 4079–4082.

(7) Matsumoto, T.; Okuno, Y.; Sugiura, Y. Specific interaction between a novel enediyne chromophore and apoprotein in macromolecular antitumor antibiotic C-1027. *Biochem. Biophys. Res. Commun.* **1993**, *195*, 659–666.

(8) Khokhlov, A. S.; Cherches, B. Z.; Reshetov, P. D.; Smiirnov, V. V.; Navashin, S. M.; Formina, I. P. Physico-chemical and biological studies on actinoxanthin, antibiotic from *Actinomyces globisporus 1131*. *J. Antibiot.* (*Tokyo*) **1969**, *22*, 541–544.

(9) Yamashita, T.; Naoi, N.; Hidaka, T.; Watanabe, K.; Kumada, Y.; Takeuchi, T.; Umezawa, H. Studies of auromomycin. *J. Antibiot.* (*Tokyo*) **1979**, *32*, 330–339.

(10) (a) Ishida, N.; Miyazaki, K.; Kumagai, K.; Rikimaru, M. Neocarzinostatin, an antitumor antibiotic of high molecular weight. *J. Antibiot.* (*Tokyo*) **1965**, *Ser. A18*, 68–76. (b) Kim, K.-H.; Kwon, B.-M.; Myers, A. G.; Rees, D. C. Crystal structure of neocarzinostatin, an antitumor protein-chromophore complex. *Science* **1993**, *262*, 1042–1046.

(11) (a) Leet, J. E.; Schroeder, D. R.; Hofstead, S. J.; Golik, J.; Colson, K. L.; Huang, S.; Klohr, S. E.; Doyle, T. W.; Matson, J. A. Kedarcidin, a new chromophore antitumor antibiotic: structure elucidation of kedarcidin chromophore. *J. Am. Chem. Soc.* **1992**, *114*, 7946–7948. (b) Leet, J. E.; Schroeder D. R.; Langley, D. R.; Colson, K. L.; Klohr, S. E.; Lee, M. S.; Golik, J.; Hofstead, S. J.; Doyle, T. W.; Matson, J. A. Chemistry and structure elucidation of kedarcidin chromophore. *J. Am. Chem. Soc.* **1993**, *115*, 8432–8443. (c) Zein, N.; Casazza, A. M.; Doyle, T. W.; Leet, J. E.; Schroeder, D. R.; Solomon, W.; Nadler, S. G. Selective proteolytic activity of the antitumor agent kedarcidin. *Proc. Natl. Acad. Sci. U.S.A.* **1993**, *90*, 8009–8012.

(12) (a) Dean, P. M.; Wakelin, L. P. G. Electrostatic components of drug-receptor recognition. I: Structural and sequence analogues of DNA polynucleotides. *Proc. R. Soc. London B* **1980**, *209*, 453–471. (b) Dean, P. M.; Wakelin, L. P. G. Electrostatic components of drug-receptor recognition. II: The DNA-binding antibiotic actinomycin. *Proc. R. Soc. London B* **1980**, *209*, 473–487. (c) Dean, P. M. Molecular recognition in drug research. *Perspect. Comput.* **1983**, *3*, 14–27. (d) Komatsu, K.; Nakamura, H.; Nakagawa, S.; Umeyama, H. Electrostatic forces in the inhibition of dihydrofolate reductase by methotrexate. A field potential study. *Chem. Pharm. Bull.* (*Tokyo*) **1984**, *32*, 3313–3316.

(13) Brooks, B. R.; Bruccoleri, R. E.; Olafson, B. D.; States, D. J.; Swaminathan, S.; Karplus, M. Charmm: A program for macromolecular energy, minimization, and dynamics calculations. *J. Comput. Chem.* **1983**, *4*, 187–217.

(14) Roey, P. V.; Beerman, T. A. Crystal structure analysis of auromomycin apoprotein (macromycin) shows importance of protein side chains to chromophore binding selectivity. *Proc. Natl. Acad. Sci. U.S.A.* **1989**, *86*, 6587–6591.

(15) Levitt, M.; Lifson, S. Refinement of protein conformations using a macromolecular energy minimization procedure. *J. Mol. Biol.* **1969**, *46*, 269–274.

(16) (a) Snyder, J. P. The cyclization of calicheamicin-esperamicin analogues: a predictive biradicaloid transition state. *J. Am. Chem. Soc.* **1989**, *111*, 7630–7632. (b) Magnus, P.; Fortt, S.; Pitterna, T.; Snyder, J. P. Synthetic and mechanistic studies on esperamicin A and calicheamicin γ_1. Molecular strain rather than π-bond proximity determines the cycloaromatization rates of bicyclo[7.3.1]enediynes. *J. Am. Chem. Soc.* **1990**, *112*, 4986–4987. Langley, D. R.; Doyle, T. W.; Beveridge, D. L. The dynamicin-DNA interaction complex. A model based on affinity cleavage and molecular dynamics simulation. *J. Am. Chem. Soc.* **1991**, *113*, 4395–4403. (d) Langrey, D. R.; Golik, J.; Krishnan, B.; Doyle, T. W.; Beveridge, D. L. The DNA-esperamicin A_1 complex. A model based on solvated molecular dynamics simulations. *J. Am. Chem. Soc.* **1994**, *116*, 15–19.

(17) Kirkpatrick, S.; Gelatt, C. D., Jr.; Vecchi, M. P. Optimization by simulated annealing. *Science* **1983**, *220*, 671–680.

(18) (a) Ueno, M.; Tanaka, T.; Hirama, M.; Imajo, S.; Ishiguro, M.; Mizugaki, M.; Edo, K.; Komatsu, H. Proton NMR studies on the chromophore binding structure in neocarzinostatin complex. *Tetrahedron Lett.* **1991**, *32*, 3175–3178. (b) Ishiguro, M.; Imajo, S.; Hirama, M. Modeling study of the structure of the macromolecular antitumor antibiotic neocarzinostatin. Origin of the stabilization of the chromophore. *J. Med. Chem.* **1991**, *34*, 2366–2373. (c) Hirama, M.; Tanaka, T.; Fujita, K.; Imajo, S.; Ishiguro, M. Solution structure of the antitumor antibiotic neocarzionostatin, a chromophore–protein complex. *J. Chem. Soc., Chem. Commun.* **1993**, 1205–1207.

(19) (a) Nicolaou, K. C.; Zuccarello, G.; Ogawa, Y.; Schweiger, E. J.; Kumazawa, T. Cyclic conjugated enediynes related to calicheamicins and esperamicins: calculations, synthesis, and properties. *J. Am. Chem. Soc.* **1988**, *110*, 4866–4868. (b) Nicolaou, K. C.; Zuccarello, G.; Riemer, C.; Estevez, V. A.; Dai, W.-M. Design, synthesis, and study of simple macrocyclic conjugated enediynes. The 10-membered ring enediyne moiety of the enediyne anticancer antibiotics. *J. Am. Chem. Soc.* **1992**, *114*, 7360–7371.

(20) Edo, K.; Saito, K.; Akiyama-Murai, Y.; Mizugaki, M. An antitumor polypeptide antibiotic neocarzinostatin: the mode of apoprotein-chromophore inteaction. *J. Antibiot.* (*Tokyo*) **1988**, *41*, 554–562.

(21) (a) Hearst, J. E.; Vinograd, J. The net hydration of deoxyribonucleic acid. *Proc. Natl. Acad. Sci. U.S.A.* **1961**, *47*, 825–830. (b) Tunis, M.-J. B.; Hearst, J. E. On the hydration of DNA. I. Preferential hydration and stability of DNA in concentrated trifluoroacetate solution. *Biopolymers* **1968**, *6*, 1325–1344. (c) Tunis, M.-J. B.; Hearst, J. E. On the hydration of DNA. II. Base composition dependence of the Net hydration DNA. *Biopolymers* **1968**, *6*, 1345–1353. (d) Falk, M.; Hartwan, Jr, K. A.; Lord, R. C. Hydoration of deoxyribonucleic acid. I. A gravimetric study *J. Am. Chem. Soc.* **1962**, *84*, 3843–3846. (e) Falk, M.; Hartwan, Jr, K. A.; Lord, R. C. Hydration of deoxyribonucleic acid. II. An infrared study. *J. Am. Chem. Soc.* **1963**, *85*, 387–391. (f) Falk, M.; Hartwan, Jr, K. A.; Lord, R. C. Hydration of deoxyribonucleic acid. III. A spectroscopic study of the effect of the hydration on the structure of deoxyribonucleic acid. *J. Am. Chem. Soc.* **1963**, *85*, 391–394.

(22) Edo, K.; Mizugaki, M.; Koide, Y.; Seto, H.; Furihata, K.; Otake, N.; Ishida, N. The structure of neocarzinostatin chromophore possessing a novel bicyclo-[7.3.0]-dodecadiyne system. *Tetrahedron Lett.* **1985**, *26*, 331–334.